

Multiple-channel wavelength conversion by use of engineered quasi-phase-matching structures in LiNbO₃ waveguides

M. H. Chou, K. R. Parameswaran, and M. M. Fejer

E. L. Ginzton Laboratory, Stanford University, Stanford, California 94305-4085

I. Brener

Bell Laboratories, Lucent Technologies, 700 Mountain Avenue, Murray Hill, New Jersey 07974

Received April 22, 1999

We report difference frequency generation-based wavelength converters with multiple phase-matching wavelengths that use engineered quasi-phase-matching structures in LiNbO₃ waveguides. Multiple-channel wavelength conversion is demonstrated within the 1.5- μ m band and between the 1.3- and 1.5- μ m bands. With simultaneous use of M pump wavelengths, these devices can also be used to perform wavelength broadcasting, in which each of N input signals is converted into M output wavelengths. © 1999 Optical Society of America
OCIS codes: 060.2330, 190.2620, 190.4360.

Nonlinear optical frequency mixing, such as four-wave mixing and difference-frequency generation, is an attractive method for wavelength conversion and dispersion compensation in wavelength-division-multiplexed optical networks.^{1,2} It can also be used to perform signal-processing functions in optical time-division-multiplexed systems.³ Such frequency-mixing processes provide a signal bandwidth of several terahertz, can simultaneously upconvert and downconvert multiple signal channels, perform spectral inversion of the signal, and add negligible spontaneous-emission noise.

Quasi phase matching (QPM) allows for tailoring of the nonlinear optical frequency-mixing process through engineerable grating structures.^{4,5} Wavelength conversion by use of QPM-difference-frequency generation has been demonstrated in AlGaAs (Ref. 1) and LiNbO₃ (Refs. 6–8) waveguides. Efficient wavelength conversion has also been demonstrated in devices based on QPM with a cascaded second-order nonlinearity [$\chi^{(2)} : \chi^{(2)}$].^{9,10} In this Letter we report multiple-channel wavelength converters that use engineered QPM structures in periodically poled LiNbO₃ waveguides, in which the application of M pumps allows for simultaneous conversion of each of N input signals to M output wavelengths (wavelength broadcast). Efficient wavelength conversion within the 1.5- μ m band and between the 1.3- and 1.5- μ m bands is demonstrated.

The difference frequency generation-based device for 1.5- μ m-band wavelength conversion uses a pump at a wavelength of \sim 780 nm. This pump at frequency ω_p mixes with a signal at frequency ω_s through the second-order nonlinearity $\chi^{(2)}$ to generate an output at shifted frequency $\omega_{out} = \omega_p - \omega_s$. Phase matching is accomplished by choice of an appropriate QPM grating period. The wavelength-tuning curve, i.e., conversion efficiency versus wavelength, for nonlinear frequency-conversion processes is related to the interacting wavelengths through the Fourier transform (FT) of the spatial distribution of the effective nonlinearity. Arbitrary wavelength-response functions can be obtained

by design of appropriate spatial grating structures. In this Letter we use QPM structures with multiple phase-matching wavelengths for wavelength-division-multiplexed wavelength conversion.

We designed structures with a phase-reversal sequence superimposed upon a uniform QPM grating, as shown in Fig. 1.⁴ The FT of the new structure can be viewed as the convolution of a sinc function (a FT of a finite uniform grating) and a comb function (with some high-order harmonics, since it is the FT of a square wave). The output power can be expressed as

$$P_{\omega_{out}} \approx \eta_{norm} P_{\omega_p} P_{\omega_s} \left| \frac{1}{L} \int_0^L \Pi(z) \exp(-j\Delta\beta_m z) dz \right|^2, \quad (1)$$

where P_{ω_p} , P_{ω_s} , and $P_{\omega_{out}}$ are the pump, input signal, and converted output powers, respectively. η_{norm} is the device's normalized efficiency in units of percent per watt. $\Delta\beta_m = 2\pi(n_p/\lambda_p - n_s/\lambda_s - n_{out}/\lambda_{out} - 1/\Lambda_{QPM})$ is the phase mismatch among the interacting waves (λ_p , λ_s , λ_{out}) and the uniform QPM grating (Λ_{QPM}). $\Pi(z)$ is the superimposed phase-reversal sequence. As an example of a two-channel device, let $\Pi(z)$ be a periodic phase-reversal sequence with a grating period of Λ_{phase} and a duty cycle of 50%. The superimposed phase-reversal sequence can be written as $\Pi(z) = \sum_{n=1}^{\infty} (2/\pi n) \sin(\pi n/2) [\exp(jK_n z) + \exp(-jK_n z)]$, where $K_n = 2\pi n/\Lambda_{phase}$. Insertion of

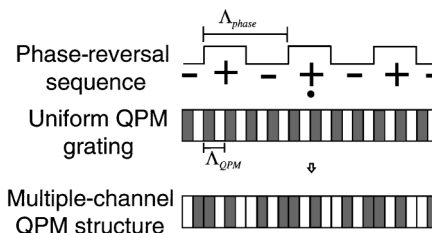


Fig. 1. Multiple-channel QPM structure formed by superimposition of a phase-reversal grating upon a uniform QPM grating.

$\Pi(z)$ into relation (1) yields

$$P_{\text{out}} \approx \eta_{\text{norm}} P_s P_p \sum_{n=1,3,5,\dots} \left(\frac{2}{\pi n} \right)^2 \left[\text{sinc}^2 \left(\frac{\Delta\beta_m + K_n}{2} L \right) + \text{sinc}^2 \left(\frac{\Delta\beta_m - K_n}{2} L \right) \right]. \quad (2)$$

This results in a tuning curve with multiple phase-matching wavelengths, whose locations and spacing can be engineered to standard wavelength-division-multiplexed channel wavelengths that conform to the International Telecommunication Union grid.

We fabricated the waveguides by annealed proton exchange in periodically poled LiNbO₃. The device includes integrated waveguide structures for efficient mode coupling⁷ and has a 42-mm-long wavelength-conversion section with a uniform QPM grating period of 14.75 μm and superimposed phase-reversal sequences. The phase-reversal period Λ_{phase} of the two-channel device is 14 mm. The three-channel device is implemented by the duty cycle of the phase-reversal sequence on a two-channel device ($\Lambda_{\text{phase}} = 7$ mm; duty cycle, 26.5%), which changes the ratio of center-channel efficiency relative to the other two channels. The four-channel device is implemented by superimposition of another phase-reversal sequence ($\Lambda_{\text{phase}} = 14$ mm) on a two-channel device ($\Lambda_{\text{phase}} = 7$ mm; the relative phase of 14-mm-period grating to the 7-mm-period grating is 0.1364π), splitting the two channels into four.

We first characterized the devices by measuring second-harmonic generation versus fundamental wavelength. Figure 2(a) shows a normalized sinc² wavelength-tuning curve for a device with a single phase-matching wavelength (channel) of 1550.4 nm and peak internal normalized efficiency (output second-harmonic-generation power divided by the square of the input pump power) of $\sim 500\%/W$. Figures 2(b), 2(c), and 2(d) show the normalized tuning curves of devices with two, three, and four phase-matching channels, respectively. The phase-matching wavelengths are centered around 1550.4 nm and separated by ~ 1.6 nm (200 GHz). The efficiency for the individual channels is $\sim 41\%$, 22% , and 17% relative to the one-channel device with the same interaction length in the two, three, and four channel devices, respectively. The unwanted phase-matching peaks can be suppressed by further optimization of grating structures.

We performed wavelength conversion, using a cw Ti-sapphire laser operating at ~ 780 nm as a pump, and chose to operate the device at $\sim 120^\circ\text{C}$ to avoid photorefractive effects. The 780-nm pump and the 1.5- μm -band signal were free-space launched into two different waveguides and combined into the wavelength-conversion section by an integrated directional coupler.⁷ Figure 3(a) shows the measured output spectrum for a single-channel device. The internal conversion efficiency is ~ -4 dB with a pump at a wavelength of 781 nm and ~ 90 mW of pump power coupled into the waveguide. Figures 3(b), 3(c), and 3(d) show the results with internal conversion

efficiencies of ~ -7 , -9 , and -10 dB for two-, three-, and four-channel devices, respectively. We obtained these curves by tuning the pump to each individual phase-matching wavelength and combining the results in the same graph, since four pump lasers were not available. However, by use of multiple pump wavelengths, these devices can convert one or more inputs to multiple output wavelengths simultaneously.

We measured the bandwidth of the wavelength converters by tuning the input signal wavelength with the pump fixed at each individual phase-matching wavelength. The 3-dB conversion bandwidth is the same (~ 56 nm) for both the single-channel device and each individual channel in the multiple-channel devices. Figure 4 shows the bandwidth of each individual channel in the one- and two-channel devices.

We also fabricated similar multiple-channel devices for wavelength conversion between the 1.3- and 1.5- μm bands.⁸ These devices have a QPM period of 12.4 μm

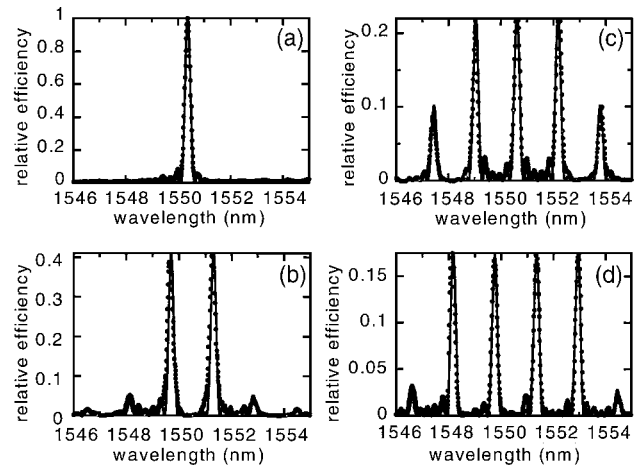


Fig. 2. SHG wavelength-tuning curves for (a) one-channel, (b) two-channel, (c) three-channel, and (d) four-channel devices. The filled circles are measured results, and the solid curves are theoretical fits. The efficiencies are relative to the peak efficiency ($\sim 500\%/W$) of a one-channel device.

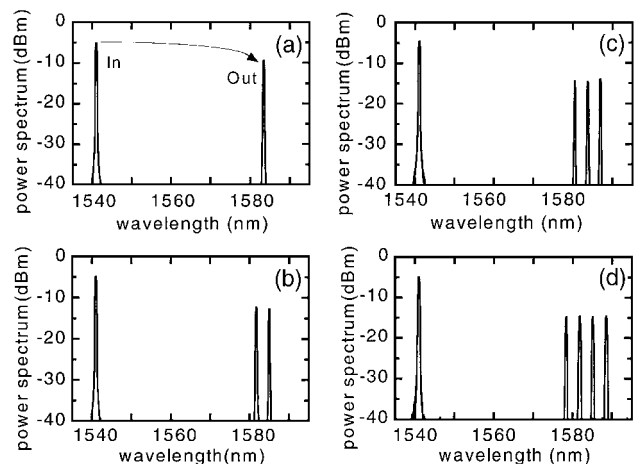


Fig. 3. Measured multiple-channel wavelength conversion of (a) one-channel, (b) two-channel, (c) three-channel, and (d) four-channel devices. Wavelength conversions of the individual channels were combined to form these plots.

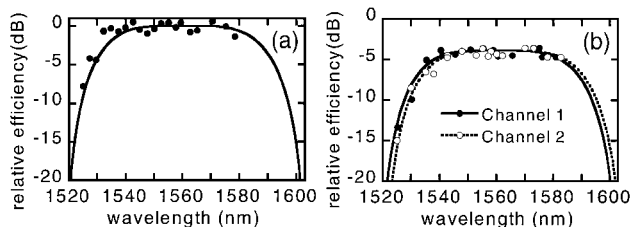


Fig. 4. Signal bandwidth of each individual channel in the (a) one-channel and (b) two-channel devices. The filled circles are measured results, and the solid curves are theoretical fits.

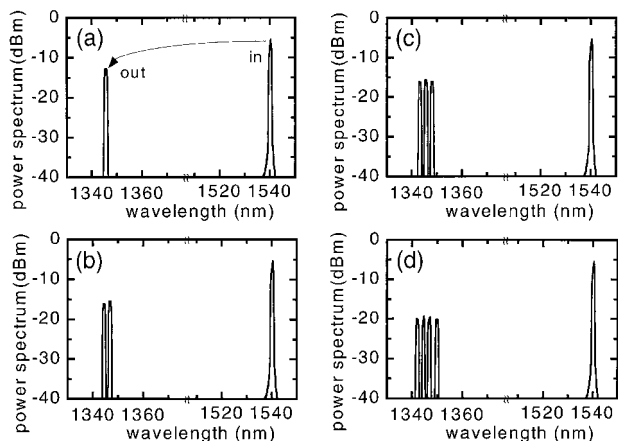


Fig. 5. 1.5–1.3- μm multiple-channel wavelength conversion of (a) one-channel, (b) two-channel, (c) three-channel, and (d) four-channel devices. These plots were formed in the same way as those in Fig. 3.

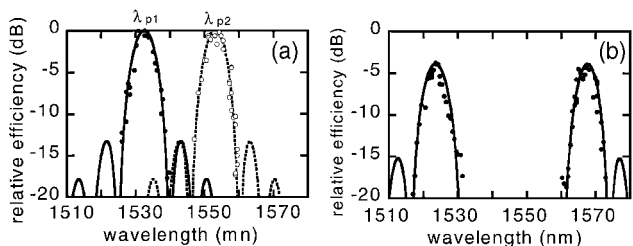


Fig. 6. Bandwidth of each individual channel for a 1.3–1.5- μm device: (a) one-channel device at two different pump wavelengths (717.9 and 718.2 nm), (b) two-channel device at a fixed pump wavelength (718.1 nm).

and a 36-mm-long wavelength-conversion section. We performed the wavelength-conversion experiment by mixing a signal at a wavelength of ~ 1540 nm and the pump from the Ti:sapphire laser at a wavelength of ~ 718 nm. Figure 5 shows the measured output spectrum that we obtained by tuning the pump wavelength to each individual phase-matching wavelength and combining the results in the same graph. The conversion efficiencies are ~ -7 , -10 , -12 , and -14 dB for the one-, two-, three-, and four-channel devices, respectively, with ~ 50 -mW pump power coupled into the waveguides. The same devices can also perform multiple-wavelength conversion from the 1.3- μm band to the 1.5- μm band.

The 1.3–1.5- μm device has a 3-dB bandwidth of ~ 6 nm, which is approximately one-tenth that in the

1.5- μm -band device. Hence with a fixed pump wavelength the device can accommodate only a limited number of signal channels for 1.3–1.5- μm conversion. The narrower bandwidth is due to the off-degenerate operation, in contrast to the near-degenerate operation for the 1.5- μm -band device. However, a very wide signal bandwidth can be obtained by use of a tunable pump, since any input signal wavelength (channel) can be phase matched to a particular pump wavelength by use of a fixed QPM period. Figure 6(a) shows the signal bandwidth of a single-channel device at two different pump wavelengths. We shifted the signal phase-matching wavelengths by ~ 20 nm by tuning the pump wavelength by ~ 0.3 nm. One can also use multiple-channel devices to obtain a range of signal bandwidths with a single pump wavelength, since each phase-matching peak allows for the generation of a separate signal band. Figure 6(b) shows the signal bands of a two-channel device that uses a pump fixed at ~ 718.1 nm.

In summary, we have demonstrated 1.5- and 1.3–1.5- μm multiple-channel wavelength converters that use engineered QPM structures in LiNbO₃ waveguides. 1.5- μm -band multiple-channel converters can also be operated by use of $\chi^{(2)} : \chi^{(2)}$, which allows for the use of a pump within the 1.5- μm -band. These devices allow for selecting the desired output wavelength by choice of an appropriate pump wavelength. Wavelength broadcast can be done by use of multiple pump wavelengths simultaneously.

This research was sponsored by the Joint Services Electronics Program, by the Defense Advanced Research Projects Agency, and by Lucent Technologies. We also thank Crystal Technology for donating LiNbO₃ substrates. M.-H. Chou's e-mail address is choumh@leland.stanford.edu.

References

1. S. J. B. Yoo, *J. Lightwave Technol.* **14**, 955 (1996).
2. U. Feiste, R. Ludwig, E. Dietrich, S. Diez, H. J. Ehrke, Dz. Razic, and H. G. Weber, *Electron. Lett.* **34**, 2044 (1998).
3. S. Kawanishi, *IEEE J. Quantum Electron.* **34**, 2064 (1997).
4. M. L. Bortz, "Quasi-phasematched optical frequency conversion in lithium niobate waveguides," Ph.D. dissertation (Stanford University, Stanford, Calif., 1994).
5. G. Imeshev, A. Galvanauskas, D. Harter, M. A. Arbore, M. Proctor, and M. M. Fejer, *Opt. Lett.* **23**, 864 (1998).
6. C. Q. Xu, H. Okayama, and M. Kawahara, *Appl. Phys. Lett.* **63**, 3559 (1993).
7. M. H. Chou, J. Hauden, M. A. Arbore, and M. M. Fejer, *Opt. Lett.* **23**, 1004 (1998).
8. M. H. Chou, K. R. Parameswaran, M. A. Arbore, J. Hauden, and M. M. Fejer, in *Conference on Lasers and Electro-Optics*, Vol. 6 of 1998 OSA Technical Digest Series (Optical Society of America, Washington, D.C., 1998), paper CThZ2.
9. C. G. Trevino-Palacios, G. I. Stegeman, P. Baldi, and M. P. De Micheli, *Electron. Lett.* **34**, 2157 (1998).
10. M. H. Chou, I. Brener, M. M. Fejer, E. E. Chaban, and S. B. Christman, *IEEE Photon. Technol. Lett.* **11**, 653 (1999).